Inverse Problems and Imaging
Volume 3, No. 1, 2009, 43–68
doi:10.3934/ipi.2009.3.43

IMAGE RECOVERY USING FUNCTIONS OF BOUNDED VARIATION AND SOBOLEV SPACES OF NEGATIVE DIFFERENTIABILITY

Yunho Kim and Luminita A. Vese

Department of Mathematics
University of California, Los Angeles
Los Angeles, CA 90095-1555, USA

(Communicated by Jean-Michel Morel)

Abstract. In this work we wish to recover an unknown image from a blurry, or noisy-blurry version. We solve this inverse problem by energy minimization and regularization. We seek a solution of the form $u + v$, where u is a function of bounded variation (cartoon component), while v is an oscillatory component (texture), modeled by a Sobolev function with negative degree of differentiability. We give several results of existence and characterization of minimizers of the proposed optimization problem. Experimental results show that this cartoon + texture model better recovers textured details in natural images, by comparison with the more standard models where the unknown is restricted only to the space of functions of bounded variation.

1. **Introduction.** We consider in this paper one of the classical problems in image analysis: the recovery of an unknown image from its blurry version, in the presence of a known blurring operator. Suppose that we are given a blurry (and possibly noisy) gray-scale image $f : \Omega \to \mathbb{R}$, where Ω is either $\mathbb{R}^n$ or an open, bounded and connected subset of $\mathbb{R}^n$. We wish to recover a clean image $\tilde{f}$ from f. Let K be a blurring operator (a linear and continuous smoothing operator, for instance a convolution with the Gaussian kernel or with the average kernel). The standard linear degradation model that relates f to $\tilde{f}$ is

$$f = K\tilde{f} + noise.$$

By our proposed method, we do not only recover a sharp image $\tilde{f}$, but we also decompose $\tilde{f}$ into the cartoon and the texture parts, which will be denoted by u and v, respectively.

The standard method for solving such inverse ill-posed problems is inspired from Tikhonov regularization [37], [38], [39], which can be written as the general minimization problem of a functional in integral form,

$$\inf_{\tilde{f}} \int_\Omega |f - K\tilde{f}|^p dx + \lambda \int_\Omega R(\tilde{f}) dx, \tag{1}$$

2000 *Mathematics Subject Classification.* Primary: 35J85, 49J40, 65M06; Secondary: 65M32.
Key words and phrases. Image restoration, variational models, bounded variation, Sobolev spaces, oscillatory functions.
This work has been supported by the National Science Foundation grants NSF-DMS 0714945, NSF-DMS 0312222, by a Beckenbach Dissertation Year Fellowship, and by the Institute for Pure and Applied Mathematics (IPAM).

where p is chosen function of the noise type (for instance, $p = 2$ for Gaussian noise, $p = 1$ for salt-and-pepper noise). The regularizing potential R is usually of the form $R(\tilde{f}) = R(|D\tilde{f}|)$, depending on partial derivatives of $\tilde{f}$, and with at most linear growth at infinity for the recovery of sharp edges. We refer in this context to an extensive work of minimization models of the form (1), with theoretical results, numerical algorithms, and experimental results: [17] (non-convex potentials R), [32] (continuation of total variation minimization from [31]), [1], [11], [5], [40], [4] for the analysis of the problem in the convex case, [19], [10], [9] with convex or non-convex regularizations, [25], [26], [27] , [14] using total variation and wavelets principles, among other examples.

More recently, model (1) has been generalized to cases of the form

$$\inf_{\tilde{f}} \|f - K\tilde{f}\|^p + \lambda \int_\Omega R(|D\tilde{f}|), \tag{2}$$

where $\|\cdot\|$ denotes the norm in a Banach space of generalized functions of negative degree of differentiability, that better model oscillatory functions (such as noise or texture). This is inspired by proposals of Y. Meyer [28] and of D. Mumford - B. Gidas [29].

Using such norms in dual spaces of distributions, for image deblurring, the work [30] imposes $\tilde{f} \in BV(\Omega)$ and $f - K\tilde{f} \in \dot{H}^{-1}(\Omega)$, and this is generalized in [23], [24] to the case $\tilde{f} \in BV(\Omega)$ and $f - K\tilde{f} \in \dot{H}^{-s}(\Omega)$, defined in terms of the Fourier transform. In these works, as in those mentioned above, the recovered image $\tilde{f}$ is represented by a function of bounded variation. However, this penalizes too much oscillatory details, such as texture. Moreover, it has been shown in [18], [2] and [3] that natural images with finer details are not well represented by functions of bounded variation.

We propose in this paper a variational deblurring model that aims to recover the unknown image $\tilde{f}$ as the sum of two components, $u + v$, where u is a function of bounded variation, representing the cartoon component, and v is a function in a Sobolev space of negative degree of differentiability (in $\dot{W}^{-s,p}$, more general than the choice $\dot{H}^{-s}$ considered in [23] , [24]). The space $\dot{W}^{-s,p}$ has been satisfactorily proposed and used by J.B. Garnett, P.W. Jones, T.M. Le and the second author in [15] to model oscillatory components in natural images, in the case $K = identity$ ([15] is an alternative way to represent oscillatory details in images, in addition to other prior work by Aujol and collaborators [6], [7], [8], Le and collaborators [21], [16], [41], Starck et al. [33], Levine, [22], or a hierarchical approach in Tadmor et al. [34], [35], among others). We will make this choice to model the oscillatory component v of the recovered image, therefore the proposed deblurring model is a continuation of the work [15]. We thus recall here the main ingredient in our model, the image decomposition model $f \approx u + v$, previously proposed in [15]:

$$\inf_{u \in BV(\Omega), v \in \dot{W}^{-s,p}(\Omega)} \mu \|f - (u+v)\|^2_{L^2(\Omega)} + |u|_{BV(\Omega)} + \lambda \|v\|_{\dot{W}^{-s,p}(\Omega)}.$$

A related prior work is by I. Daubechies and G. Teschke [12], where the authors also recover an image from its blurry version by the following "cartoon + texture" minimization model

$$\inf_{u \in B^1_{1,1}(\Omega), v \in H^{-1}(\Omega)} \mu \|f - K(u+v)\|^2_{L^2(\Omega)} + |u|_{B^1_{1,1}(\Omega)} + \lambda \|v\|^2_{H^{-1}(\Omega)}, \tag{3}$$

in the Besov-wavelets framework. Very satisfactory results are reported in [12], where the recovered sharp image is given by $\tilde{f} = u + v$.

We also recall the earlier L. Rudin - S. Osher model [32] for image deblurring using the total variation (as an extension of the TV denoising model proposed by L. Rudin - S. Osher - E. Fatemi [31]): given a degradation model of the form $f = Ku + noise$, the authors [32] have proposed to recover a sharp image u in the presence of a blurring operator K and noise, by the minimization

$$\inf_{u \in BV(\Omega)} \mu \|f - Ku\|^2_{L^2(\Omega)} + \int_\Omega |Du|, \tag{4}$$

where the last term denotes the total variation of u, to be defined in the next section.

We will show numerical comparisons between our proposed model and the above Rudin-Osher model (4), that we solve using a finite differences discretization of the following Euler-Lagrange equation with time dependence and gradient descent: $u(0,x) = f(x)$ in Ω, and

$$\frac{\partial u}{\partial t} = 2\mu K^*(f - Ku) + \mathrm{div}\Big(\frac{Du}{|Du|}\Big) \text{ in } (0,\infty)\times\Omega, \qquad \frac{\partial u}{\partial \vec{n}} = 0 \text{ on } (0,\infty)\times\partial\Omega, \tag{5}$$

where $\vec{n}$ denotes the exterior unit normal to $\partial\Omega$. We will see that the recovery of the unknown image using a $u + v$ (cartoon + texture) model gives better results and more textured details, than using only a cartoon model u. A recent work on image deblurring using regularized locally-adaptive kernel regression in a variational approach is by Takeda, Farsiu and Milanfar [36], with very satisfactory results shown on several experiments.

The outline of the paper is as follows: Section 2 is devoted to the necessary definitions and the description of the proposed deblurring-denoising model. Section 3 contains several theoretical results and remarks regarding the existence and the characterization of minimizers. Finally, Section 4 gives the Euler-Lagrange equations associated with the optimization problem based on alternating minimization and the numerical algorithm, while Section 5 presents numerical results and comparisons with models given in [32, 12, 36]. We note that a short and preliminary version of this work has been published in the SPIE Electronic Imaging 2008 conference proceedings [20].

2. Description of the proposed model.

Before we introduce our proposed minimization model for image restoration, we need the necessary definitions of the function spaces that will be used.

Definition 2.1. We say that a function $u : \Omega \to \mathbb{R}$ is a function of bounded variation, $u \in BV(\Omega)$, if and only if $u \in L^1(\Omega)$ and

$$\int_\Omega |Du| := \sup\Big\{ \int_\Omega u \mathrm{div}\phi dx : \ \phi \in C^1_c(\Omega, \mathbb{R}^n), \ \|\phi\|_\infty \le 1 \Big\} < \infty.$$

The space $W^{1,1}(\Omega)$ is a subspace of $BV(\Omega)$, and for $u \in W^{1,1}(\Omega)$ we have $\int_\Omega |Du| = \int_\Omega |Du(x)|dx$, where now Du is the usual distributional gradient in $L^1(\Omega, \mathbb{R}^n)$. The Banach space $BV(\Omega)$ is equipped with the following norm, which extends the classical norm in $W^{1,1}(\Omega)$:

$$\|u\|_{BV(\Omega)} = \|u\|_{L^1(\Omega)} + \int_\Omega |Du|.$$

We will also use the notation $|u|_{BV(\Omega)}$ for the semi-norm $\int_\Omega |Du|$. The space $BV(\Omega)$ will be used to model the cartoon component u of the recovered deblurred image $\tilde{f}$.

To model the texture component v, we use the Sobolev spaces $\dot{W}^{-s,p}$, $s > 0$, $p \geq 1$, that do not penalize oscillations in images. Since these spaces for $s \in \mathbb{R}$ are defined in terms of the Fourier transform, we have to assume that the data is defined in $\mathbb{R}^n$ (obtained by extension by zero outside of the fundamental domain Ω, or by periodicity when Ω is a rectangle). However, we will still use the notation $\dot{W}^{-s,p}(\Omega)$.

Definition 2.2. The homogeneous Sobolev space $\dot{W}^{s,p}(\Omega)$ for $s \in \mathbb{R}$, $1 \leq p \leq \infty$ on a fundamental domain Ω is defined by

$$\dot{W}^{s,p}(\Omega) = \Big\{ v : |\nabla|^s v \in L^p \Big\},$$

where $|\nabla|^s v(x) := ((2\pi|\cdot|)^s \widehat{v}(\cdot))^\vee(x)$ in $\Omega = \mathbb{R}^n$ (or if Ω is a periodic domain then we use the discrete Fourier transform), with the norm on the quotient (homogeneous) space

$$\|v\|_{\dot{W}^{s,p}(\Omega)} = \|((2\pi|\cdot|)^s \widehat{v}(\cdot))^\vee\|_{L^p}.$$

Note that $|\nabla|^s v$ is defined in terms of the Fourier and the inverse Fourier transforms. There is a corresponding kernel to the operator $|\nabla|^s$, denoted by k_s, i.e.,

$$|\nabla|^s v = k_s * v.$$

For instance, when $s = 2$, we have $|\nabla|^2 v = \Delta v$.

As mentioned in the introduction, in the work [15] by J. Garnett, P. Jones, T. Le and the second author of the present paper, the authors proposed an image decomposition model

$$f \approx u + v,$$

where u is the cartoon part and $v = \Delta g$ for some $g \in \dot{W}^{-\alpha+2,p}$ is the texture or noise part. The homogeneous Sobolev spaces of functions with negative degree of differentiability turned out to be a good choice to model texture. Notice that $\Delta(\dot{W}^{-\alpha+2,p}) = \dot{W}^{-\alpha,p}$. Inspired by this model, we consider the following degradation model for image recovery in the presence of blur and noise:

$$f = K(u + v) + r = k * (u + v) + r,$$

where $v = \Delta g$ for some $g \in \dot{W}^{-\alpha+2,p}$ and r is a small residual. $u + v = u + \Delta g$ will be our recovered deblurred image, and this can be done by minimizing the following proposed functional

$$\mathcal{F}(u, g) = |u|_{BV(\Omega)} + \mu \int_\Omega |f - k * (u + \Delta g)|^2 dx + \lambda \|g\|_{\dot{W}^{s,p}(\Omega)}, \tag{6}$$

where k is a standard convolution kernel (such as the Gaussian kernel or the average kernel) that models the blurring operator, and $\mu, \lambda > 0$, $s \geq 0$, $s = -\alpha + 2$. If there is no noise in the data, then we can choose sufficiently large μ to ensure $r = f - k * (u + \triangle g) \approx 0$, dx-a.e.; if additive noise of zero mean and known variance $\sigma^2 > 0$ is also present, then we choose μ so that the variance of the computed residual $r = f - k * (u + \triangle g)$ is very close to σ^2.

3. Minimizers of the functional $\mathcal{F}$.

In this section we state and prove several theoretical results of existence, uniqueness and characterization of minimizers for the proposed model.

3.1. **Existence of a minimizer for $1 < p \leq \infty$.** The problem is to minimize the following functional,

$$\begin{aligned}\mathcal{F}(u,g) &= |u|_{BV(\Omega)} + \mu \int_\Omega |f - k*u - k*\Delta g|^2 dx + \lambda \|\Delta g\|_{\dot{W}^{\alpha,p}(\Omega)} \\ &= |u|_{BV(\Omega)} + \mu \int_\Omega |f - k*u - k*\Delta g|^2 dx + \lambda \|g\|_{\dot{W}^{s,p}(\Omega)},\end{aligned}$$

and we first wish to establish existence of minimizers when $1 < p < \infty, \mu > 0, \lambda > 0$,.

Here and in what follows, $-2 \leq \alpha < 0$, $s = \alpha + 2$ and $\overline{\Omega} = [0, M] \times [0, N] \subset \mathbb{R}^2$ will be the fundamental domain of the periodic domain such as T^2 (extension to higher dimensions can be treated in the same way). We assume that $f \in L^2(\Omega)$. We begin by showing existence of minimizers assuming stronger conditions on the kernel k; then these will be relaxed.

Thus, suppose first that $1 < p < \infty$ and the kernel k is in $\dot{W}^{2-s,q}(\Omega)$, where p and q are conjugate exponents. Notice that

$$k * \Delta g = |\nabla|^{2-s} k * |\nabla|^s g.$$

Since $|\nabla|^{2-s} k \in L^q(\Omega)$ and $|\nabla|^s g \in L^p(\Omega)$, then $k * \triangle g$ is bounded. So $k * \Delta g \in L^2(\Omega)$.

Now for $\epsilon > 0$, let $k_\epsilon \in \dot{W}^{2-s,q}(\Omega) \cap L^1(\Omega)$ with $\int_\Omega k_\epsilon = 1$. We define

$$\mathcal{F}_\epsilon(u,g) = |u|_{BV(\Omega)} + \mu \int_\Omega |f - k_\epsilon * u - k_\epsilon * \Delta g|^2 dx + \lambda \|g\|_{\dot{W}^{s,p}(\Omega)}. \tag{7}$$

Theorem 3.1. *The functional $\mathcal{F}_\epsilon$ from (7) has a minimizer (u^ϵ, g^ϵ) in $BV(\Omega) \times \dot{W}^{s,p}(\Omega)$ such that*

$$\mathcal{F}_\epsilon(u^\epsilon, g^\epsilon) = \inf_{u \in BV(\Omega), g \in \dot{W}^{s,p}(\Omega)} \mathcal{F}_\epsilon(u,g).$$

Proof. If we choose $u = g \equiv 0$, we have that $\mathcal{F}_\epsilon(u,g) < \infty$. Also, the functional is always bounded from below by zero. Therefore the infimum is finite and we can consider $(u_n^\epsilon, g_n^\epsilon)$ a minimizing sequence. Thus there is $0 < C < \infty$ such that $\mathcal{F}_\epsilon(u_n^\epsilon, g_n^\epsilon) < C$ for all n. Since $\Delta g_n^\epsilon \in \dot{W}^{\alpha,p}(\Omega)$, with $\alpha < 0$, we may assume that $\int_\Omega k_\epsilon * \Delta g_n^\epsilon dx = 0$. We may also assume that $\int_\Omega u_n^\epsilon dx = \int_\Omega f dx$ since if not, by changing u_n^ϵ to $u_n^\epsilon + \frac{\int_\Omega (f - k_\epsilon * u_n^\epsilon) dx}{|\Omega|}$ we have

$$\mathcal{F}_\epsilon\Big(u_n^\epsilon + \frac{\int_\Omega (f - k_\epsilon * u_n^\epsilon) dx}{|\Omega|},\ g_n^\epsilon\Big) \leq \mathcal{F}_\epsilon(u_n^\epsilon, g_n^\epsilon).$$

Note that $\frac{\int_\Omega \left(u_n^\epsilon + \frac{\int_\Omega (f - k_\epsilon * u_n^\epsilon) dx}{|\Omega|}\right) dx}{|\Omega|} = \frac{\int_\Omega f(x) dx}{|\Omega|}$. By Poincaré-Wirtinger inequality, we know that

$$\|u_n^\epsilon - (u_n^\epsilon)_\Omega\|_{L^2(\Omega)} \leq C' |u_n^\epsilon|_{BV(\Omega)},$$

where $(u_n^\epsilon)_\Omega = \Big(\int_\Omega u_n^\epsilon(x) dx\Big)/|\Omega| = \Big(\int_\Omega f(x) dx\Big)/|\Omega|$ and $C' > 0$ is a constant. Therefore the sequence u_n^ϵ is also bounded in $L^1(\Omega)$, thus the sequence u_n^ϵ is bounded in $BV(\Omega)$, which means that there is $u^\epsilon \in BV(\Omega)$ such that $u_n^\epsilon \to u^\epsilon$ in $L^1(\Omega)$ and $|u^\epsilon|_{BV(\Omega)} \leq \liminf_{n\to\infty} |u_n^\epsilon|_{BV(\Omega)}$ (passing to subsequences if necessary, still denoted in the same way).

The sequence $\{g_n^\epsilon\}$ is bounded in $\dot{W}^{s,p}(\Omega)$, which means that $\{|\nabla|^s g_n\}$ is bounded in $L^p(\Omega)$. Hence, there exists $\tilde{g} \in L^p(\Omega)$ such that $|\nabla|^s g_n \rightharpoonup \tilde{g}$ in $L^p(\Omega)$, i.e.,

$$g_n^\epsilon \rightharpoonup g^\epsilon \quad \text{in } \dot{W}^{s,p}(\Omega),$$

where $g^\epsilon = |\nabla|^{-s}\tilde{g}$. This implies that $|\nabla|^{2-s}k_\epsilon * |\nabla|^s g_n^\epsilon \to |\nabla|^{2-s}k_\epsilon * |\nabla|^s g^\epsilon$ pointwise. Also for all n,

$$\||\nabla|^{2-s}k_\epsilon * |\nabla|^s g_n^\epsilon\|_\infty \le \||\nabla|^{2-s}k_\epsilon\|_q \||\nabla|^s g_n^\epsilon\|_p \le \frac{C}{\lambda}\||\nabla|^{2-s}k_\epsilon\|_q < \infty.$$

Thus, since $|\nabla|^{2-s}k_\epsilon * |\nabla|^s g_n^\epsilon$ is uniformly bounded on a bounded domain, it is uniformly bounded in $L^2(\Omega)$. We finally obtain

$$k_\epsilon * \Delta g_n^\epsilon = |\nabla|^{2-s}k_\epsilon * |\nabla|^s g_n^\epsilon \to |\nabla|^{2-s}k_\epsilon * |\nabla|^s g^\epsilon = k_\epsilon * \Delta g^\epsilon \quad \text{in } L^2(\Omega)$$

(notice that we obtain strong convergence in $L^2(\Omega)$). Therefore,

$$\mathcal{F}_\epsilon(u^\epsilon, g^\epsilon) \le \liminf_{n\to\infty} \mathcal{F}_\epsilon(u_n^\epsilon, g_n^\epsilon) = \inf_{u,g} \mathcal{F}_\epsilon(u, g).$$

□

Now we choose a C^∞ function φ with compact support in Ω satisfying $\int_\Omega \varphi(x)dx = 1$, $\varphi \ge 0$ and define $\varphi_\epsilon(x) = \epsilon^{-2}\varphi(x/\epsilon)$. We then have $\int_\Omega \phi_\epsilon(x)dx = 1$ also. Suppose that $k \in L^1(\Omega)$ with $\int_\Omega k(x)dx = 1$. Then $k_\epsilon = k * \varphi_\epsilon \to k$ in $L^1(\Omega)$ and $k_\epsilon \in \dot{W}^{2-s,q}(\Omega) \cap L^1(\Omega)$. In what follows, we will be using this k_ϵ for any given $k \in L^1(\Omega)$.

Lemma 3.2. *With the kernels k and k_ϵ just described, for any pair $(u, g) \in BV(\Omega) \times \dot{W}^{s,p}(\Omega)$ satisfying $\mathcal{F}(u, g) < \infty$, we have*

$$\lim_{\epsilon\to 0} \mathcal{F}_\epsilon(u, g) = \mathcal{F}(u, g) < \infty.$$

Proof. Since $\mathcal{F}(u, g) < \infty$, we know that $k * u,\ k * \Delta g \in L^2(\Omega)$. We have

$$\begin{aligned}
&|\mathcal{F}_\epsilon(u, g) - \mathcal{F}(u, g)| \\
=&\mu\Big|\|f - k_\epsilon * (u + \Delta g)\|^2_{L^2(\Omega)} - \|f - k * (u + \Delta g)\|^2_{L^2(\Omega)}\Big| \\
\le&\mu\Big(\|f - k_\epsilon * (u + \Delta g)\|_{L^2(\Omega)} + \|f - k * (u + \Delta g)\|_{L^2(\Omega)}\Big) \\
&\qquad \cdot \|(k_\epsilon - k) * (u + \Delta g)\|_{L^2(\Omega)}.
\end{aligned}$$

It suffices to see that $\|(k_\epsilon - k) * (u + \Delta g)\|_{L^2(\Omega)} \to 0$ as $n \to \infty$. Indeed,

$$\begin{aligned}
&\|(k_\epsilon - k) * (u + \Delta g)\|_{L^2(\Omega)} \le \|(k_\epsilon - k) * u\|_{L^2(\Omega)} + \|(k_\epsilon - k) * \Delta g\|_{L^2(\Omega)} \\
\le\ &\|(k * u) * \varphi_\epsilon - k * u\|_{L^2(\Omega)} + \|(k * \Delta g) * \varphi_\epsilon - (k * \Delta g)\|_{L^2(\Omega)} \to 0 \quad \text{as } n \to \infty.
\end{aligned}$$

□

Let's go back to the original problem, and denote

$$A := \inf_{u\in BV(\Omega), g\in\dot{W}^{s,p}(\Omega)} \mathcal{F}(u, g) < \infty.$$

We can now prove the following existence theorem for our problem.

Theorem 3.3. *Let $\mu, \lambda > 0$, $-2 \le \alpha < 0$, $s = 2 + \alpha$, $1 < p < \infty$, $k \in L^1(\Omega)$ with $\int_\Omega k(x)dx = 1$, and $f \in L^2(\Omega)$. The minimization problem*

$$\inf_{u\in BV(\Omega), g\in\dot{W}^{s,p}(\Omega)} \mathcal{F}(u, g) = |u|_{BV(\Omega)} + \mu\int_\Omega |f - k*u - k*\Delta g|^2 dx + \lambda\|g\|_{\dot{W}^{s,p}(\Omega)} \tag{8}$$

has at least one solution.

Proof. Let (u_n, g_n) be a minimizing sequence. Lemma 3.2 says that there exists a sequence ϵ_n such that $\epsilon_n \to 0$ as $n \to \infty$, $\epsilon_n \geq \epsilon_{n+1}$ and

$$\left|\mathcal{F}_{\epsilon_n}(u_n, g_n) - \mathcal{F}(u_n, g_n)\right| < 2^{-n}.$$

Then

$$A = \lim_{n\to\infty} \mathcal{F}_{\epsilon_n}(u_n, g_n) < \infty.$$

Without loss of generality, we assume that there exists $0 < C < \infty$ such that for all n,

$$0 \leq \mathcal{F}_{\epsilon_n}(u_n, g_n) \leq C.$$

Instead of dealing with (u_n, g_n), we will deal with another sequence $(u_n^{\epsilon_n}, g_n^{\epsilon_n})$, each of which is a minimizer of

$$\inf_{u\in BV(\Omega), g\in \dot{W}^{s,p}(\Omega)} \mathcal{F}_{\epsilon_n}(u, g),$$

that is, for each n

$$(u_n^{\epsilon_n}, g_n^{\epsilon_n}) = \arg\min_{u\in BV(\Omega), g\in \dot{W}^{s,p}(\Omega)} \mathcal{F}_{\epsilon_n}(u, g).$$

For simplicity, we let $w_n = u_n^{\epsilon_n}$, $h_n = g_n^{\epsilon_n}$, $\varphi_n = \varphi_{\epsilon_n}$, $k_n = k_{\epsilon_n}$ and $\mathcal{F}_n = \mathcal{F}_{\epsilon_n}$. With the same argument as before, we can extract a subsequence w_n so that there exists $u_0 \in BV(\Omega)$ with $w_n \rightharpoonup u_0$ in $BV - w*$. Note that for all n,

$$\mathcal{F}_n(w_n, h_n) \leq \mathcal{F}_n(u_n, g_n),$$

i.e.,

$$\limsup_{n\to\infty} \mathcal{F}_n(w_n, h_n) \leq \lim_{n\to\infty} \mathcal{F}_n(u_n, g_n) = A.$$

Since $\sup_n \mathcal{F}_n(w_n, h_n) \leq C$, we have

$$\sup_n \|k_n * \Delta h_n\|_{L^2(\Omega)} = \sup_n \|k * \varphi_n * \Delta h_n\|_{L^2(\Omega)} < \infty,$$

i.e., there exists $\rho \in L^2(\Omega)$ such that for an appropriate subsequence $k_n * \Delta h_n$,

$$k_n * \Delta h_n = k * \varphi_n * \Delta h_n \rightharpoonup \rho \quad \text{in } L^2(\Omega). \tag{9}$$

On the other hand,

$$\|\varphi_n * \Delta h_n\|_{\dot{W}^{\alpha,p}(\Omega)} = \|\varphi_n * h_n\|_{\dot{W}^{s,p}(\Omega)} = \|\varphi_n * |\nabla|^s h_n\|_{L^p(\Omega)}$$
$$\leq \|\varphi_n\|_{L^1(\Omega)} \||\nabla|^s h_n\|_{L^p(\Omega)} = \||\nabla|^s h_n\|_{L^p(\Omega)} = \|h_n\|_{\dot{W}^{s,p}(\Omega)} \leq C/\lambda < \infty.$$

Hence, there exists $g_0 \in \dot{W}^{s,p}(\Omega)$ such that for an appropriate subsequence $\varphi_n * h_n$,

$$\varphi_n * h_n \rightharpoonup g_0 \quad \text{in } \dot{W}^{s,p}(\Omega), \quad \text{i.e.,} \quad \varphi_n * \Delta h_n = \Delta\varphi_n * h_n \rightharpoonup \Delta g_0 \quad \text{in } \dot{W}^{\alpha,p}(\Omega). \tag{10}$$

Note that since $\|\varphi_n * h_n\|_{\dot{W}^{s,p}(\Omega)} \leq \|h_n\|_{\dot{W}^{s,p}(\Omega)}$,

$$\|g_0\|_{\dot{W}^{s,p}(\Omega)} \leq \liminf_{n\to\infty} \|h_n\|_{\dot{W}^{s,p}(\Omega)}.$$

Let $B = \{v \in C^\infty(\Omega) : v \text{ has compact support in } \Omega\}$. B is a dense subset in $L^t(\Omega)$ and in $\dot{W}^{s,t}(\Omega)$ for any $1 < t < \infty$. If $v \in B$, then $k * v$ is in $\dot{W}^{-\alpha,q}(\Omega)$. By (10) with a notation $\bar{k}(x) = k(-x)$,

$$\lim_{n\to\infty} \int_\Omega (k_n * \Delta h_n) v dx = \lim_{n\to\infty} \int_\Omega (k * (\varphi_n * \Delta h_n)) v dx$$
$$= \lim_{n\to\infty} \int_\Omega (\varphi_n * \Delta h_n)(\bar{k} * v) dx = \int_\Omega \Delta g_0 (\bar{k} * v) dx = \int_\Omega (k * \Delta g_0) v dx.$$

On the other hand, for $v \in B$, by (9),

$$\lim_{n\to\infty} \int_\Omega (k_n * \Delta h_n) v dx = \int_\Omega \rho v dx.$$

Hence, for all $v \in B$,

$$\int_\Omega \rho v dx = \int_\Omega (k * \Delta g_0) v dx.$$

Since

$$\begin{aligned} \|k * \Delta g_0\|_{L^2(\Omega)} &= \sup\Big\{ \int_\Omega (k * \Delta g_0) v dx : v \in B,\ \|v\|_{L^2(\Omega)} = 1 \Big\} \\ &= \sup\Big\{ \int_\Omega \rho v dx : v \in B,\ \|v\|_{L^2(\Omega)} = 1 \Big\} = \|\rho\|_{L^2(\Omega)} < \infty, \end{aligned}$$

we finally have $k_n * \Delta h_n \rightharpoonup k * \Delta g_0$ in $L^2(\Omega)$ and $k * \Delta g_0 \in L^2(\Omega)$. Now the following inequalities are satisfied:

$$\mathcal{F}(u_0, g_0) \le \liminf_{n\to\infty} \mathcal{F}_n(w_n, h_n) \le \limsup_{n\to\infty} \mathcal{F}_n(w_n, h_n) \le A = \inf_{u\in BV, g\in \dot{W}^{s,p}} \mathcal{F}(u, g).$$

Therefore, $(u_0, g_0) \in BV(\Omega) \times \dot{W}^{s,p}(\Omega)$ is a minimizer of the original problem

$$\inf_{u\in BV(\Omega), g\in \dot{W}^{s,p}(\Omega)} \mathcal{F}(u, g).$$

□

Remark 1. The property $\int_\Omega k(x)dx = 1$ (which is a standard normalization of the blurring kernel and not a too restrictive assumption) is necessary to show that for a minimizing sequence (u_n, g_n), the means $\int_\Omega u_n(x)dx$ are bounded, which enabled us to find a $BV - w*$ limit u_0 using the Poincaré-Wirtinger inequality. So if $\int_\Omega k(x)dx = \beta > 0$, then we can change k to $\frac{1}{\beta}k$, f to $\frac{1}{\beta}f$ and μ to $\beta\mu$, and we can apply the above theorem.

Remark 2. When $p = \infty$, the theorem also remains true since the weak-$*$ convergence in $L^\infty(\Omega)$ guarantees that we can still find the weak-$*$ limit and in the end we can pass to the limit to obtain a minimizer.

3.2. **Characterization of minimizers.** By the previous Remark 1, here and in what follows we will assume that $|\Omega| = 1$ and $\int_\Omega k(x)dx = 1$. We prove in this section additional properties of minimizers of problem (8) related to uniqueness issues and a characterization using dual residual norm inspired from prior work [28], [4], [21] and [35]. Note that our functional in (8) is convex, but not strictly convex in the pair variable (u, g). Thus, we may expect non-uniqueness of its minimizers and it is natural to consider the set of all minimizers. Therefore, we first introduce some notations to simplify the next statements and characterizations.

Definition 3.4. We denote the set of all minimizers of problem (8) by $\mathcal{M}$, thus

$$\mathcal{M} = \Big\{ (u, g) \in BV(\Omega) \times \dot{W}^{s,p}(\Omega) : \mathcal{F}(u, g) = \inf_{(v,h)\in BV(\Omega)\times \dot{W}^{s,p}(\Omega)} \mathcal{F}(v, h) \Big\},$$

and also a subset $\mathcal{M}' \subset \mathcal{M}$ by

$$\mathcal{M}' = \Big\{ (u, g) \in \mathcal{M} : |u|_{BV(\Omega)} \neq 0 \quad \text{or} \quad \|g\|_{\dot{W}^{s,p}(\Omega)} \neq 0 \Big\}.$$

Note that $\mathcal{M}$ is a nonempty set, based on the existence Theorem 3.3. We have also introduced the set $\mathcal{M}'$ of non-trivial minimizers (e.g. minimizers (u, g) different from $(constant, 0)$). We will be able to say under which conditions a trivial pair $(constant, 0)$ is a minimizer or not. We will define on $L^2(\Omega)$ a "residual oscillatory norm" $\|\cdot\|_{*,\lambda}$ dual to the $BV + \dot{W}^{s,p}$ norms (with $\|\cdot\|_{*,\lambda}$ small for very rough, oscillatory functions), such that if $\|f - f_\Omega\|_{*,\lambda}$ is small, then a trivial pair is a minimizer, or all of $f - f_\Omega$ goes into the residual $f - k(u + \triangle g)$; if $\|f - f_\Omega\|_{*,\lambda}$ is not that small, then a trivial pair cannot be a minimizer. In other words, we will see later that the assertion "either $\mathcal{M} = \mathcal{M}'$ or $\mathcal{M} = \mathcal{M}' \cup \{(f_\Omega, 0)\}$" is true (where f_Ω denotes the mean of f over Ω).

• We first look at uniqueness-like properties of the functional. Since the functional $\mathcal{F}$ is convex, for $(u_1, g_1), (u_2, g_2) \in \mathcal{M}$ and $0 < t < 1$,

$$\mathcal{F}(tu_1 + (1-t)u_2, tg_1 + (1-t)g_2) \le t\mathcal{F}(u_1, g_1) + (1-t)\mathcal{F}(u_2, g_2).$$

As a matter of fact, we have for $0 < t < 1$,

$$\mathcal{F}(tu_1 + (1-t)u_2, tg_1 + (1-t)g_2) = t\mathcal{F}(u_1, g_1) + (1-t)\mathcal{F}(u_2, g_2). \tag{11}$$

Theorem 3.5. *Let $1 < p < \infty$. For $(u_1, g_1), (u_2, g_2) \in \mathcal{M}'$, there exists $m > 0$ such that*

$$k * (u_1 + \Delta g_1) = k * (u_2 + \Delta g_2), \tag{12}$$

$$\Delta g_1 = m \Delta g_2. \tag{13}$$

Proof. By (11), we know that for $0 < t < 1$,

$$\begin{aligned} &|f - (tk * (u_1 + \Delta g_1) + (1-t)k * (u_2 + \Delta g_2))|^2 \\ &= t|f - k * (u_1 + \Delta g_1)|^2 + (1-t)|f - k * (u_2 + \Delta g_2)|^2. \end{aligned}$$

Since the mapping $x \mapsto x^2$ is strictly convex, this implies that

$$f - k * (u_1 + \Delta g_1) = f - k * (u_2 + \Delta g_2) \quad a.e.,$$

and therefore we obtain (12). Also by the fact that Minkowski inequality becomes equality if and only if the functions are linearly dependent, we know that there exists $m > 0$ such that

$$|\nabla|^s g_1 = m|\nabla|^s g_2 \quad a.e.,$$

which implies (13). □

• Next, we analyze further the set of minimizers $\mathcal{M}$ introducing the dual "rougher" norm $\|\cdot\|_{*,\lambda}$ and the possibility of having, or not, a trivial minimizer (outside $\mathcal{M}'$ or not).

Definition 3.6. Given a function $w \in L^2(\Omega)$ and $\lambda > 0$, we define

$$\|w\|_{*,\lambda} = \sup_{u \in BV(\Omega),\ g \in \dot{W}^{s,p}(\Omega),\ |u|_{BV(\Omega)} \neq 0 \text{ or } \|g\|_{\dot{W}^{s,p}(\Omega)} \neq 0} \frac{\langle w,\ k * (u + \Delta g)\rangle}{|u|_{BV(\Omega)} + \lambda \|g\|_{\dot{W}^{s,p}(\Omega)}} \le \infty, \tag{14}$$

where $\langle \cdot, \cdot \rangle$ is the inner product in $L^2(\Omega)$.

Remark 3. Note that if $\int_\Omega w \neq 0$, then $\|w\|_{*,\lambda} = \infty$.

Theorem 3.7. *Let $f \in L^2(\Omega)$ and $1 < p < \infty$. Also let $f_\Omega = \Big(\int_\Omega f(x)dx\Big)/|\Omega|$. Then each $(u_0, g_0) \in \mathcal{M}'$ satisfies*

$$|u_0|_{BV(\Omega)} = 2\mu\langle f - k * (u_0 + \Delta g_0), k * u_0\rangle, \tag{15}$$

$$\|g_0\|_{\dot{W}^{s,p}(\Omega)} = \tfrac{2\mu}{\lambda}\langle f - k * (u_0 + \Delta g_0), k * \Delta g_0\rangle. \tag{16}$$

Furthermore,

1. *$\|f - f_\Omega\|_{*,\lambda} \le \frac{1}{2\mu}$ if and only if $(f_\Omega, 0) \in \mathcal{M}$.*
2. *If $\|f - f_\Omega\|_{*,\lambda} > \frac{1}{2\mu}$, then $(u_0, g_0) \in \mathcal{M}'$ if and only if it satisfies the following additional condition together with (15), (16) :*

$$\Big\|f - k * (u_0 + \Delta g_0)\Big\|_{*,\lambda} = \frac{1}{2\mu}. \tag{17}$$

Proof. Let's first prove 1. Suppose that $\|f - f_\Omega\|_{*,\lambda} \le \frac{1}{2\mu}$. For any $u \in BV(\Omega),\ g \in \dot{W}^{s,p}(\Omega)$,

$$\langle f - f_\Omega,\ k * (u + \Delta g)\rangle \le \frac{1}{2\mu}(|u|_{BV(\Omega)} + \lambda\|g\|_{\dot{W}^{s,p}(\Omega)}),$$

i.e.,

$$0 \le |u|_{BV(\Omega)} + \lambda\|g\|_{\dot{W}^{s,p}(\Omega)} + 2\mu\langle f - f_\Omega,\ -k * (u + \Delta g)\rangle$$

or

$$\begin{aligned}&\mu\textstyle\int_\Omega |f - f_\Omega|^2 dx + \mu\int_\Omega |k * (u + \Delta g)|^2 dx\\ &\le |u|_{BV(\Omega)} + \lambda\|g\|_{\dot{W}^{s,p}(\Omega)} + \mu\textstyle\int_\Omega |f - f_\Omega - k * (u + \Delta g)|^2 dx.\end{aligned}$$

Hence, for any $u \in BV(\Omega),\ g \in \dot{W}^{s,p}(\Omega)$,

$$\mathcal{F}(f_\Omega, 0) = \mu\int_\Omega |f - k * (f_\Omega)|^2 dx = \mu\int_\Omega |f - f_\Omega|^2 dx \le \mathcal{F}(u + f_\Omega, g),$$

which means that $(f_\Omega, 0) \in \mathcal{M}$. For the opposite direction, assume $(f_\Omega, 0) \in \mathcal{M}$. Then for any $u \in BV(\Omega)$, any $g \in \dot{W}^{s,p}(\Omega)$ and $\epsilon > 0$, we have

$$\mathcal{F}(f_\Omega, 0) = \mu\int_\Omega |f - f_\Omega|^2 dx \le \mathcal{F}(\epsilon u + f_\Omega, \epsilon g).$$

After division by $\epsilon > 0$, we obtain

$$0 \le |u|_{BV(\Omega)} + \lambda\|g\|_{\dot{W}^{s,p}(\Omega)} - 2\mu\langle f - f_\Omega,\ k * (u + \Delta g)\rangle + \epsilon\mu\int_\Omega |k * (u + \Delta g)|^2 dx.$$

Letting $\epsilon \downarrow 0$, we obtain

$$\langle f - f_\Omega,\ k * (u + \Delta g)\rangle \le \frac{1}{2\mu}(|u|_{BV(\Omega)} + \lambda\|g\|_{\dot{W}^{s,p}(\Omega)}).$$

Since $u \in BV(\Omega)$ and $g \in \dot{W}^{w,p}(\Omega)$ are arbitrary, we deduce

$$\|f - f_\Omega\|_{*,\lambda} \le \frac{1}{2\mu}.$$

For the direct implication of 2, to show (15) and (16), we first let $(u_0, g_0) \in \mathcal{M}'$. Then for any $g \in \dot{W}^{s,p}(\Omega)$,

$$\mathcal{F}(u_0, g_0) \le \mathcal{F}(u_0, g),$$

i.e.,

$$\begin{aligned}\lambda\|g_0\|_{\dot{W}^{s,p}(\Omega)} &\leq \lambda\|g\|_{\dot{W}^{s,p}(\Omega)} + 2\mu\int_\Omega (f - k*(u_0+\Delta g_0))k*(\Delta g_0 - \Delta g)dx \\ &+ \mu\int_\Omega |k*(\Delta g_0 - \Delta g)|^2 dx. \end{aligned} \tag{18}$$

If $g = (1-\epsilon)g_0$ for $0 < \epsilon < 1$, then by letting $\epsilon \downarrow 0$ we get

$$\|g_0\|_{\dot{W}^{s,p}(\Omega)} \leq \frac{2\mu}{\lambda}\int_\Omega (f - k*(u_0+\Delta g_0))k*\Delta g_0 dx.$$

On the other hand, if $g = (1+\epsilon)g_0$ for $0 < \epsilon$, then by letting $\epsilon \downarrow 0$ we obtain

$$\|g_0\|_{\dot{W}^{s,p}(\Omega)} \geq \frac{2\mu}{\lambda}\int_\Omega (f - k*(u_0+\Delta g_0))k*\Delta g_0 dx.$$

Hence we obtain (16). Similarly for any $u \in BV(\Omega)$,

$$\mathcal{F}(u_0, g_0) \leq \mathcal{F}(u, g_0),$$

i.e.,

$$|u_0|_{BV(\Omega)} \leq |u|_{BV(\Omega)} + 2\mu\int_\Omega (f - k*(u_0+\Delta g_0))k*(u_0-u)dx + \mu\int_\Omega |k*(u_0-u)|^2 dx. \tag{19}$$

If we let $u = (1-\epsilon)u_0$ for $0 < \epsilon < 1$ and take $\epsilon \downarrow 0$, and then we let $u = (1+\epsilon)u_0$ for $0 < \epsilon$ and take $\epsilon \downarrow 0$ again, then we obtain (15).

To finalize the direct implication of 2, suppose that $\|f - f_\Omega\|_{*,\lambda} > \frac{1}{2\mu}$. For $(u_0, g_0) \in \mathcal{M}'$, if we add (15) and (16), we obtain

$$|u_0|_{BV(\Omega)} + \lambda\|g_0\|_{\dot{W}^{s,p}(\Omega)} = 2\mu\int_\Omega (f - k*(u_0+\Delta g_0))k*(u_0+\Delta g_0)dx,$$

which implies that

$$\Big\|f - k*(u_0+\Delta g_0)\Big\|_{*,\lambda} \geq \frac{1}{2\mu}.$$

Also if we use $g = g_0 + \epsilon h$ and $u = u_0 + \epsilon v$ in (18) and (19) with $\epsilon > 0$ and add them together and let $\epsilon \downarrow 0$, then

$$|v|_{BV(\Omega)} + \lambda\|h\|_{\dot{W}^{s,p}(\Omega)} \geq 2\mu\int_\Omega (f - k*(u_0+\Delta g_0))k*(v+\Delta h)dx.$$

Since $v \in BV(\Omega)$ and $h \in \dot{W}^{s,p}(\Omega)$ are arbitrary, we end up with the reverse inequality,

$$\Big\|f - k*(u_0+\Delta g_0)\Big\|_{*,\lambda} \leq \frac{1}{2\mu},$$

thus we obtain (17).

Conversely, let $(u_0, g_0) \in BV(\Omega) \times \dot{W}^{s,p}(\Omega)$ satisfy (15), (16) and (17). For any $u \in BV(\Omega)$ and $g \in \dot{W}^{s,p}(\Omega)$,

$$\begin{aligned}\mathcal{F}(u_0+u, g_0+g) &= |u_0+u|_{BV(\Omega)} + \lambda\|g_0+g\|_{\dot{W}^{s,p}(\Omega)} \\ &+\mu\int_\Omega |f - k*((u_0+u) + \Delta(g_0+g))|^2 dx.\end{aligned}$$

By (17),

$$|u_0+u|_{BV(\Omega)} + \lambda\|g_0+g\|_{\dot{W}^{s,p}(\Omega)} \geq 2\mu\langle f - k*(u_0+\Delta g_0),\ k*((u_0+u)+\Delta(g_0+g))\rangle.$$

By this and (15), (16),

$$\begin{aligned}\mathcal{F}(u_0+u,g_0+g) \geq & 2\mu\langle f-k*(u_0+\Delta g_0),\ k*((u_0+u)+\Delta(g_0+g))\rangle \\ & +\mu\int_\Omega |f-k*((u_0+\Delta g_0)+(u+\Delta g))|^2dx \\ = & |u_0|_{BV(\Omega)}+\lambda\|g_0\|_{\dot{W}^{s,p}(\Omega)}+\mu\int_\Omega |f-k*(u_0+\Delta g_0)|^2dx \\ & +\mu\int_\Omega |k*(u+\Delta g)|^2dx \geq \mathcal{F}(u_0,g_0),\end{aligned}$$

which means that $(u_0,g_0)\in\mathcal{M}$. If $(u_0,g_0)\notin\mathcal{M}'$, then $|u_0|_{BV(\Omega)}=0=\|g_0\|_{\dot{W}^{s,p}(\Omega)}$, i.e., $(u_0,g_0)=(f_\Omega,0)$, which contradicts our assumption $\|f-f_\Omega\|_{*,\lambda}>\frac{1}{2\mu}$. Therefore, $(u_0,g_0)\in\mathcal{M}'$. □

Remark 4. This theorem says that if $\|f-f_\Omega\|_{*,\lambda}\leq 1/(2\mu)$, then $\mathcal{M}=\mathcal{M}'\cup\{(f_\Omega,0)\}$ and if $\|f-f_\Omega\|_{*,\lambda}>1/(2\mu)$, then $\mathcal{M}=\mathcal{M}'$.

4. **The numerical minimization algorithm.** For our computational part, we assume that the given image f is a periodic function defined in $\mathbb{R}^2$ whose periodic domain is 2Ω, where $\overline{\Omega}=[0,1]\times[0,1]$. For the practical calculation of the Euler-Lagrange equations, we assume that we work with functions $u\in W^{1,1}(\Omega)$, thus $|u|_{BV(\Omega)}:=\int_\Omega |Du(x)|dx$ and Du is the distributional gradient as a function in $L^1(\Omega;\mathbb{R}^2)$. Moreover, this restriction is not too strong, since any $BV(\Omega)$ function can be approximated by a sequence of functions in $W^{1,1}(\Omega)$ in the strong topology $L^1(\Omega)$. We will formally compute the Euler-Lagrange equations associated with the optimization problem, using alternating minimization. If (u,g) is a minimizer of the functional $\mathcal{F}$, then for any $v\in W^{1,1}(\Omega)\subset BV(\Omega)$ and for any $w\in\dot{W}^{s,p}(\Omega)$:

$$\begin{aligned} - & \int_\Omega v\cdot\mathrm{div}\Big(\frac{Du}{|Du|}\Big)dx+2\mu\int_\Omega (k*v)\cdot(k*(u+\Delta g)-f)dx \\ + & \ 2\mu\int_\Omega (k*\Delta w)\cdot(k*(u+\Delta g)-f)dx \\ + & \ \lambda\int_\Omega \|k_s*g\|_p^{1-p}(|k_s*g|^{p-2}k_s*g)\cdot k_s*w dx=0.\end{aligned}$$

We solve this by using a gradient descent method and a finite difference scheme, i.e., we solve the following time-dependent system of PDE's:

$$\frac{\partial u}{\partial t} = \mathrm{div}\Big(\frac{Du}{|Du|}\Big)+2\mu k^**(f-k*(u+\Delta g)), \tag{20}$$

$$\frac{\partial g}{\partial t} = 2\mu\Delta k^**(f-k*(u+\Delta g))-\lambda\|k_s*g\|_p^{1-p}k_s*(|k_s*g|^{p-2}k_s*g) \tag{21}$$

where k^* is the transpose of k and the periodicity characterizes the boundary conditions. Since the full periodic domain is 2Ω, when we compute the Sobolev norm we should use the full domain 2Ω. Note that

$$\|g\|^p_{\dot{W}^{s,p}(\Omega)}=\frac{1}{4}\|\tilde{g}\|^p_{\dot{W}^{s,p}(2\Omega)}$$

where $\tilde{g}$ is the periodic function whose periodic domain is 2Ω and $\tilde{g}\Big|_\Omega=g$. Thus, when we compute the second term in (21), we use $\tilde{g}$ instead of g and obtain the values on Ω. Also, the Sobolev norm will be computed using the Fast Fourier Transform (FFT) since the space itself is defined in terms of the Fourier and the inverse Fourier

transforms. Recall that the Sobolev kernel k_s was defined by $\widehat{k_s}(\xi) := (2\pi|\xi|)^s$ in the continuous case. Even if we work in the discrete case, we can still use this definition since we use a square domain and we can encode the constant multiplication in the parameter λ. To obtain the numerical result, we run the algorithm until we reach a possible minimizer which will be a point after which the energy functional becomes stationary. As we will see in the next section, this model works very well in the case of deblurring without noise.

In the presence of additive noise, in the experiments, we assume that we know the variance of the noise σ^2. So, as in [4], we adjust the parameter μ after each iteration, in such a way that the energy functional is being minimized while keeping the fidelity term comparable with the noise variance. The parameter μ can be seen as a Lagrange multiplier for the constraint $\|f - k * (u + \triangle g)\|^2_{L^2(\Omega)} = \sigma^2$. Thus, we adjust the parameter μ in the following way: let $V(u,g) = \frac{\int_\Omega |f-k*u-k*\Delta g|^2 dx}{|\Omega|}$, σ^2 the noise variance, γ a small threshold parameter, then (recall $|\Omega| = 1$):

1. With initial $\mu, \lambda > 0$, especially small μ, we approximate a minimizer (u_0, g_0) using the coupled system of time-dependent partial differential equations (20)-(21).
2. If $|V(u_0, g_0) - \sigma^2| < \gamma$, then we stop.
3. If $|V(u_0, g_0) - \sigma^2| \geq \gamma$ and $V(u_0, g_0) > \sigma^2$, then we update μ by $\mu + V(u_0, g_0) - \sigma^2$.
4. If $|V(u_0, g_0) - \sigma^2| \geq \gamma$ and $V(u_0, g_0) < \sigma^2$, then we update μ by $\mu + \rho^m(V(u_0, g_0) - \sigma^2)$, where ρ is a fixed constant throughout the process and m counts the number of consecutive drops of the value $V(u_0, g_0)$ below σ^2.
5. Go to 1. with the updated μ.

The values of μ over iterations tend to an optimal choice $\mu(\sigma)$.

Remark 5. When we consider a noisy case with known noise variance σ^2, we look for a minimizer (u, g) for which the fidelity term of our model matches the variance of the noise, σ^2. Let $\lambda > 0$ be fixed and $\sigma^*(\mu)$ be defined by

$$\sigma^*(\mu) = \|f - k * (u_\mu + \Delta g_\mu)\|_{L^2(\Omega)},$$

where (u_μ, g_μ) is a minimizer of

$$\inf_{u \in BV(\Omega), g \in \dot{W}^{s,p}(\Omega)} \mathcal{F}(u, g) = |u|_{BV(\Omega)} + \mu \int_\Omega |f - k * u - k * \Delta g|^2 dx + \lambda \|g\|_{\dot{W}^{s,p}(\Omega)}.$$

Equation (12) shows that this function $\sigma^* : \mathbb{R}_+ \to \mathbb{R}_+$ is well-defined. In fact, it is easy to see that the function σ^* is non-increasing, as in [4] for the case without texture norm. Hence, if we start the algorithm with small $\mu > 0$, then we expect to have the initial computed $\sigma^*(\mu) > \sigma$; then, as we increase μ, we know that $\sigma^*(\mu)$ will decrease, until we reach the desired value σ. In this way, we are able to adjust μ in such a way that the value $\sigma^*(\mu)$ eventually becomes σ.

The numerical discretization of the partial differential equations (20) and (21) will be as follows: we will use a semi-implicit scheme to calculate u^{n+1} and an explicit scheme for g^{n+1}. We fix $\Delta x = \Delta y = h = 1$, and (i, j) will be an arbitrary

spatial grid point in the interior of the domain. Let

$$\begin{aligned}
c_0^n(i,j) &= \sqrt{(u^n(i+1,j)-u^n(i,j))^2+(u^n(i,j+1)-u^n(i,j))^2+\epsilon},\\
c_-^n(i,j) &= \sqrt{(u^n(i,j)-u^n(i-1,j))^2+(u^n(i-1,j+1)-u^n(i-1,j))^2+\epsilon},\\
c_+^n(i,j) &= \sqrt{(u^n(i+1,j-1)-u^n(i,j-1))^2+(u^n(i,j)-u^n(i,j-1))^2+\epsilon},\\
c_n(i,j) &= \frac{2}{c_0^n(i,j)}+\frac{1}{c_-^n(i,j)}+\frac{1}{c_+^n(i,j)},\\
d_1^n(i,j) &= f(i,j)-\sum_{a,b}k(a,b)(u(i-a,j-b)+\Delta g(i-a,j-b)),\\
d_2^n(i,j) &= \sum_{\sigma,\tau}k^*(\sigma,\tau)d_1^n(i-\sigma,j-\tau).
\end{aligned}$$

We have included a small $\epsilon>0$ to make sure that all the values are strictly positive in the denominators. For (20), we have

$$u^{n+1}(i,j)=\frac{u^n(i,j)+\Delta t\Big(\frac{u^n(i+1,j)+u^n(i,j+1)}{c_0^n}+\frac{u^n(i-1,j)}{c_-^n}+\frac{u^n(i,j-1)}{c_+^n}+2\mu d_2^n(i,j)\Big)}{1+c_n(i,j)\Delta t}.$$

To calculate $k_s*g(i,j)$, we use FFT and IFFT as follows: SHIFT is responsible for translation to have the center at the origin and ISHIFT is the inverse of SHIFT. When we apply FFT, we apply it to the function $\tilde{g}$ with full periodic domain 2Ω and finally select the data at those points (i,j) in the domain Ω:

$$\begin{aligned}
k_s*g(i,j) &= IFFT\Big(ISHIFT\Big(\Big(2\pi\sqrt{\xi_1^2+\xi_2^2}\Big)^s SHIFT(FFT(\tilde{g}))(\xi_1,\xi_2)\Big)\Big)(i,j)\\
h(i,j) &= |k_s*g(i,j)|^{p-2}k_s*g(i,j).
\end{aligned}$$

Now for (21), we have

$$g^{n+1}(i,j)=g_{i,j}^n+\triangle t\Big[2\mu\Delta d_2^n(i,j)-\lambda\Big(\sum_{a,b}|k_s*g^n(i,j)|^p\Big)^{1-p}k_s*h^n(i,j)\Big].$$

As usual, the Laplacian $\Delta d_2^n(i,j)$ is computed by

$$\Delta d_2^n(i,j)=d_2^n(i+1,j)+d_2^n(i-1,j)+d_2^n(i,j+1)+d_2^n(i,j-1)-4d_2^n(i,j).$$

Since the deconvolution problem, especially in the presence of noise, can be numerically highly unstable, and since we use semi-implicit and explicit schemes, the choice of $\triangle t$ implicitly depends on a CFL-like condition.

5. **Numerical results and comparisons.** We show in this section several experimental results for deblurring and denoising real images. We also analyze in practice the quality of restoration function of parameters and we present comparisons with the model (4)-(5) by Rudin-Osher from [32], with the model (3) by Daubechies-Teschke [12], and with results included in [36] by Takeda, Farsiu and Milanfar.
Deblurring. Figure 1 shows blurry data images f_1, f_2 and f_3 to be tested, and their original versions. The original images have been artificially blurred by convolution with a blurring kernel k. To obtain blurry image f_1, a 7×7 averaging kernel k was used, and for the blurry images f_2 and f_3, a 5×5 averaging kernel k was used.

In Fig. 2 we show deblurring results using the proposed model and comparisons with the Rudin-Osher model [32]. To recover sharp images from the blurry images f_1, f_2 and f_3, we have tested several parameters and we have obtained that the Sobolev space $\dot{W}^{0.1,1.3}$ was a good choice to model g, which means that the texture

Figure 1. Left: three original images; right: their blurry versions f_1 (SNR=8.9183), f_2 (SNR=7.8599), f_3 (SNR=10.2671).

part $v = \Delta g$ belongs to $\dot{W}^{-1.9,1.3}$. The tuning parameters μ and λ for the three images are set to be $\mu = 10$, $\lambda = 0.05$. Using the original clean images, we compute the SNR (Signal-to-Noise-Ratio), and we compare with the Rudin-Osher model [32]. The parameters for the Rudin-Osher model were also obtained to have the best possible results, $\triangle t = 0.01$, $\mu = 100$, and the number of iterations is 2000, 3000 and 1500 for f_1, f_2 and f_3 respectively (for both models in the case without noise, the SNR increases with iterations). SNR values are also given in the caption of Fig. 2, showing that the proposed model recovers better textured images from their blurry versions.

FIGURE 2. Deblurring results. 1st row: cartoon u; 2nd row: texture $v = \triangle g$; 3rd row: recovered images $u + v$ by BV/Sobolev model (SNR=22.6316, 22.7535, 28.1160); 4th row: recovered images by RO model [32] (SNR=15.5319, 14.7255, 21.0735).

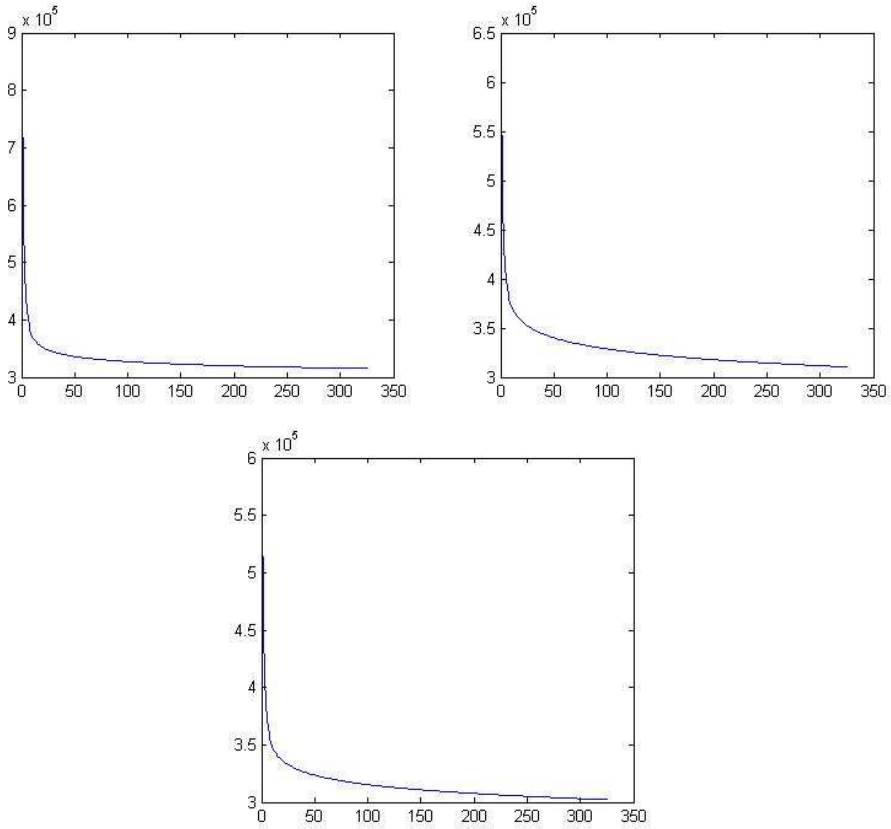

FIGURE 3. Numerical energy versus iterations for each of the three data f_1, f_2 and f_3, illustrating that the proposed numerical algorithm is stable in practice.

We show in Figure 3 plots of the numerical energy decrease versus iterations for the three experiments with the proposed model, to illustrate that our numerical implementation is stable in practice.

In the next tables and figures we show additional results for the data f_1 obtained with the proposed BV/Sobolev model and give the corresponding SNR, to see the effect of changing some of the parameters, while keeping the others fixed.

Table 1 compares the SNR values for the recovered images of the blurry image f_1 with various choices of the homogeneous Sobolev space modeling the texture component. Since we consider $-2 \leq \alpha < 0$ ($0 \leq s < 2$), we chose for the comparison $s = 0,\ 0.1,\ 0.6,\ 1$ and $p = 1,\ 1.3,\ 2,\ 3$ for 5000 and 10000 iterations, while keeping $\mu = 11$, $\lambda = 0.06$ and $\triangle t = 0.03$ fixed. The SNR value for (s_1, p_1) is better than that for (s_2, p_2) when $s_1 = \alpha_1 + 2$, $s_2 = \alpha_2 + 2$ and $-2 \leq \alpha_1 \leq \alpha_2 < 0$, $1 \leq p_2 \leq p_1$. This confirms our expectation that if the Sobolev space that we use to model textures has weaker differentiability condition, then this space better models the oscillatory component. Since we obtained the best result with $s = 0$ ($\alpha = -2$), we now fix $s = 0$ and vary $p = 1, 1.3, 2, 3, 10, 25$ to see the effect of the choice of the p values. Table 2 shows this comparison. Hence, we can expect to have the best results with

	5000 iterations				10000 iterations			
	$p=1$	$p=1.3$	$p=2$	$p=3$	$p=1$	$p=1.3$	$p=2$	$p=3$
$s=0$	18.399	21.626	21.671	21.672	17.316	22.830	22.927	22.930
$s=0.1$	16.305	21.551	21.668	21.671	15.424	22.647	22.923	22.929
$s=0.6$	X	17.133	21.525	21.658	X	17.109	22.646	22.902
$s=1$	X	12.841	19.295	21.137	X	12.776	19.4656	21.761

TABLE 1. SNR values for the recovered images from the blurry data f_1 after 5000 iterations and 10000 iterations with various choices for (s,p) and fixed $\lambda=11$, $\mu=0.06$, $\triangle t=0.03$. Recall that $s=\alpha+2$. "X" = no convergence.

	$p=1$	$p=1.3$	$p=2$	$p=3$	$p=10$	$p=25$
5000 iterations	18.3998	21.6269	21.6710	21.6724	21.6723	21.6724
10000 iterations	17.3166	22.8307	22.9278	22.9306	22.9313	22.9315

TABLE 2. SNR values for the recovered images from the blurry data f_1 after 5000 iterations and 10000 iterations with varying $p=1,1.3,2,3,10,25$ and fixed $s=0$, $\lambda=11$, $\mu=0.06$, $\triangle t=0.03$.

Iterations	5000	10000	20000	60000	70000
SNR	21.6724	22.9315	24.2301	26.3649	26.6509

TABLE 3. SNR values for the recovered images from the blurry data f_1 obtained with $s=0$, $p=25$, $\lambda=11$, $\mu=0.06$, $\triangle t=0.03$ and increasing number of iterations.

$s=0$ and large p values in the numerical computations (note that larger p gives a choice closer to the choice suggested by Y. Meyer [28], $\dot{W}^{-1,\infty}$). Fig. 4 illustrates that a much larger p improves the results for the Barbara image f_1, comparing the two recovered images ($\alpha=-1.9$ and $p=1.3$, and $\alpha=-2$ and $p=25$). Also, note that larger exponent p removes a small artifact introduced by our proposed model: to introduce texture in non-textured regions.

Table 3 shows how the SNR values of the recovered images obtained with the parameters $s=0, p=25, \mu=11, \lambda=0.06, \triangle t=0.03$ change as the number of iterations increase; thus, in the deblurring case (no noise), more iterations gives better results.

Finally, Table 4 shows how the results and SNR change function of the parameter λ, the weight of the texture norm. As expected, we can conclude that if λ is very large, then the proposed model becomes almost the Rudin-Osher model, since the allowed texture becomes too small due to a too strong weight. Fig. 5 shows the corresponding textured components $v=\triangle g$ obtained for the four λ values. We think that too large λ produces a texture component of smaller contrast.

Denoising-deblurring. We consider next restoration in the presence of both blur and noise, assuming that we know the noise variance σ^2 and updating the coefficient μ as explained before, with threshold $\gamma=\sigma/10$.

Fig. 6 shows the image restoration in the presence of noise. The noisy blurry image f_4 was taken from [36] for comparison. An 11×11 Gaussian kernel with

FIGURE 4. Comparison between small p and large p for the Barbara image f_1. Left: recovered image shown in Fig. 2 using $\dot{W}^{-1.9,1.3}$. Right recovered image using $\dot{W}^{-2,25}$.

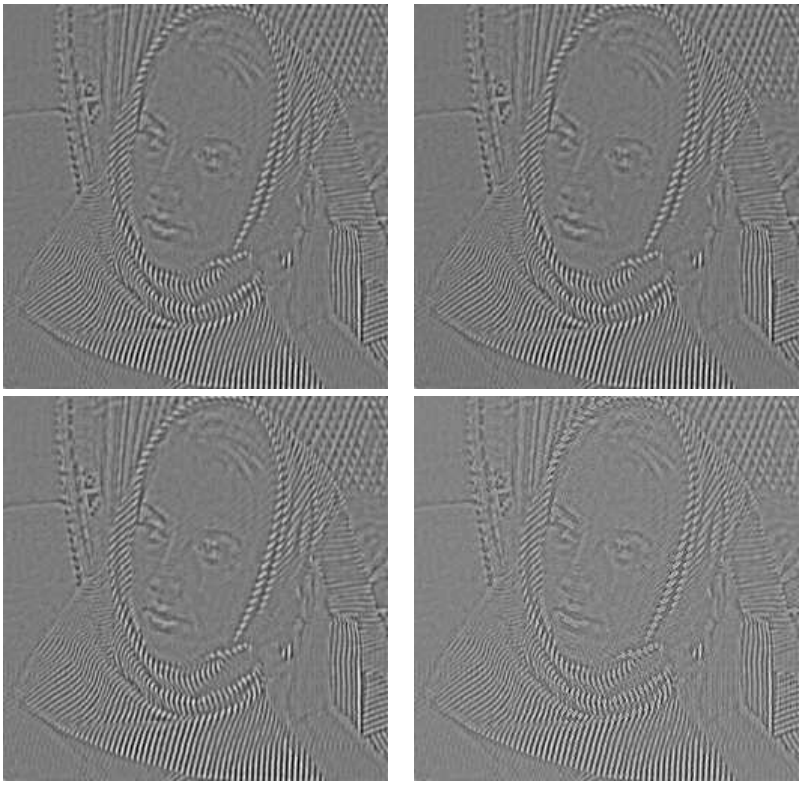

FIGURE 5. Recovered texture parts $v = \triangle g$ corresponding to Table 4. Top left: $\lambda = 0.00035$; top right: $\lambda = 0.06$; bottom left: $\lambda = 10$; bottom right: $\lambda = 1600$.

λ	0.00035	0.06	10	1600
SNR	21.6722	21.6724	21.6413	17.3048

TABLE 4. SNR values for the recovered images from the blurry data f_1 after 5000 iterations with different λ values, keeping $\mu = 11$, $s = 0$, $p = 25$, $\triangle t = 0.03$ fixed.

standard deviation 1.75 was used for blurring and then noise of standard deviation $\sigma = 1.1531$ was added. The recovered image by the proposed model from Fig. 6 bottom right has RMSE (root mean square error) 8.86, which is slightly smaller than the RMSE of other results obtained by various models presented on the webpage of P. Milanfar and related with reference [36][1]. Also to recover this clean image from the noisy blurred image f_4, the Sobolev space $\dot{W}^{0,1}$ was used, which means that the texture part $v = \Delta g$ is modeled by $\dot{W}^{-2,1}$. The initial parameters μ and λ were set to be $\mu = 4$, $\lambda = 0.02$. Using the original clean image, we can also compute the SNR (Signal-to-Noise-Ratio), which is 13.5818. Fig. 6 shows also its cartoon + texture decomposition, and a comparison with the RO model (Fig. 6 bottom left) obtained with the best optimal parameters. Again, we notice improvement of the proposed model over the RO model.

As pointed out by the referees, the problem of deconvolution, especially in the presence of noise, is a highly ill-posed problem, solved in general by regularization. However, the texture norm used in this work is not a regularizing norm (only the BV semi-norm has regularizing effects). Thus, it is natural to ask how well the proposed model can recover textured images from blurry and noisy images, with increased amount of noise. We expect that, as the noise becomes stronger and stronger, less accurate recovery is obtained. We illustrate this experiment in Fig. 7, where we have applied our BV/Sobolev model to the chemical plant image with noise of increasing standard deviation, $\sigma = 1.1531$ (same image f_4 as before), $\sigma = 3$ and $\sigma = 5$. The threshold $\gamma = \sigma/10$ to stop the process described before was used. As expected, more noise gives smaller SNR and larger RMSE. More instability can occur if the noise is stronger. Fig. 8 shows the true noise of standard deviation $\sigma = 3$ and the residual or computed noise $f - k * (u + \Delta g)$ for the noisy plant image with $\sigma = 3$. The standard deviation of the computed noise $f - k * (u + \Delta g)$ is 2.8226, very close to 3. The two images in Figure 8 were scaled with the same scaling factor so that we could better see the differences. It can be easily seen that the computed "noise" residual still contains details.

We conclude this section with a final experimental result in Fig. 9 and we show comparison with a result by Daubechies-Teschke from [12] using the model (3), where the $\dot{H}^{-1}$ norm is used to model textures in the wavelet domain. The size of the image is 256×256. The authors in [12] defined a Gaussian blurring kernel in the Fourier domain. On the other hand, our discretization uses blurring kernels defined in the spatial domain, which led us to apply the Inverse Fourier Transform (IFFT) to the kernel defined in the Fourier domain to obtain a blurring kernel defined in the spatial domain. This kernel is also Gaussian of size 256×256. We did not truncate this kernel even though the values are almost 0 outside a patch of size 13×13 centered at the origin. 4000 iterations have been applied for our proposed algorithm, with $s = 0$, $p = 5$, $\mu = 15$, $\lambda = 0.1$, $\triangle t = 0.02$. We visually notice that

[1] http://www.soe.ucsc.edu/~htakeda/AKTV.htm

Figure 6. (Left column) Top: original image. Middle: blurry-noisy data f_4 (SNR=8.9781, RMSE=15.0602). Bottom: restored using RO model (SNR=13.1432, RMSE=9.3234). (Right column) Top: cartoon u. Middle: texture $v = \triangle g$. Bottom: restored $u + v$ using BV/Sobolev model (SNR=13.5818, RMSE=8.8643).

our proposed algorithm, which is more general and allows the choice among several Sobolev spaces, gives an improved result $u + v$, recovering much more texture.

6. **Conclusion.** We have proposed a "cartoon+texture" minimization model to recover images degraded by blur, or by blur & noise. The cartoon component u

FIGURE 7. Left column, top to bottom: blurry noisy images with increasing amount of noise (noise standard deviation $\sigma = 1.1531$, $\sigma = 3$, $\sigma = 5$). Right column, top to bottom: corresponding recovered images using the proposed BV/Sobolev model: SNR=13.5818, RMSE=8.8643 ($\sigma = 1.1531$, $s = 0$, $p = 1$). SNR = 11.8415, RMSE=10.8308 ($\sigma = 3$, $s = 0$, $p = 3$). SNR = 10.6843, RMSE=12.3742 ($\sigma = 5$, $s = 0$, $p = 3$).

is modeled by a function of bounded variation, while the texture $v = \triangle g$ is modeled by a function in the Sobolev space of negative differentiability, $\dot{W}^{\alpha,p}(\Omega)$, with $-2 \leq \alpha < 0$. The recovered image is $u + \triangle g$. In the case of blur degradation only (no noise), the recovery works very well, and the residual $f - k * (u + \Delta g)$ goes to 0

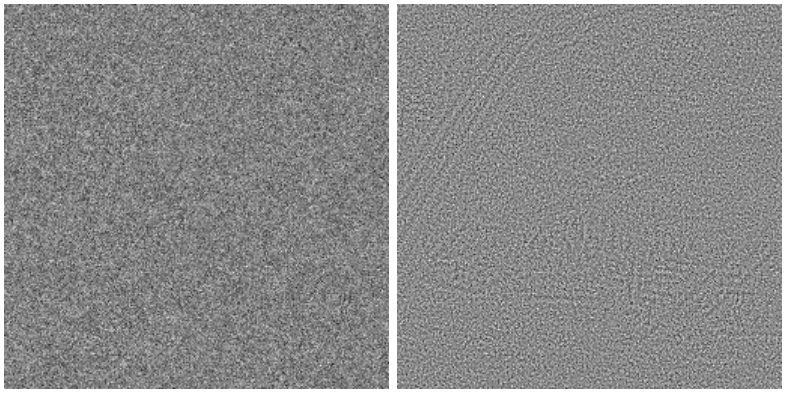

FIGURE 8. Left: true noise of standard deviation $\sigma = 3$ used in the noisy image denoted f from Fig. 7 middle left. Right: computed noise (residual $f - k * (u + \Delta g)$) obtained by the proposed BV/Sobolev model, with computed standard deviation $\sigma = 2.8226$.

as the number of iterations increases (the homogeneous Sobolev spaces of negative differentiability encourages oscillations, unlike L^p spaces, $p \geq 1$ or the space of functions of bounded variation). As expected, using $\alpha = -2$, which imposes the least amount of differentiability on the homogeneous Sobolev spaces presented the best results among $-2 \leq \alpha < 0$. Also, larger exponent p produced better results (making sure that the choice of $\triangle t$ guarantees a stable algorithm). On the other hand, in the presence of noise, which is considered to be highly oscillatory, the texture component modeled in a homogeneous Sobolev space of negative differentiability can attract noise as well. However, if the noise is small enough, then this model is able to recover important oscillatory parts. Comparisons with existing models [32], [12], [36] show that the proposed model gives improvement.

Acknowledgments. The authors would like to thank the anonymous referees for their very useful comments and suggestions that helped to improve the quality and the presentation of the manuscript, and Gerd Teschke for providing us the data and result from Fig. 9 presented in [12].

REFERENCES

[1] R. Acar and C. R. Vogel, *Analysis of bounded variation penalty methods for ill-posed problems*, Inverse problems, **10** (1994), 1217–1229.

[2] L. Alvarez, Y. Gousseau and J.-M. Morel, *Scales in natural images and a consequence on their bounded variation norm*, LNCS, **1682** (1999), 247–258.

[3] L. Alvarez, Y. Gousseau and J.-M. Morel, *The size of objects in natural and artificial images*, Advances in Imaging and Electron Physics, **111** (1999), 167–242.

[4] F. Andreu-Vaillo, V. Caselles and J. M. Mazón, "Parabolic Quasilinear Equations Minimizing Linear Growth Functionals," Birkhäuser Verlag, Progress in Mathematics , Vol., **223**, 2004.

[5] G. Aubert and L. Vese, *A variational method in image recovery*, SIAM Journal on Numerical Analysis, **34** (1997), 1948–1979.

[6] J. F. Aujol, G. Aubert, L. Blanc-Féraud and A. Chambolle, *Image decomposition into a bounded variation component and an oscillating component*, Journal of Mathematical Imaging and Vision, **22** (2005), 1–88.

[7] J. F. Aujol and A. Chambolle, *Dual norms and image decomposition models*, International Journal of Computer Vision, **63** (2005), 85–104.

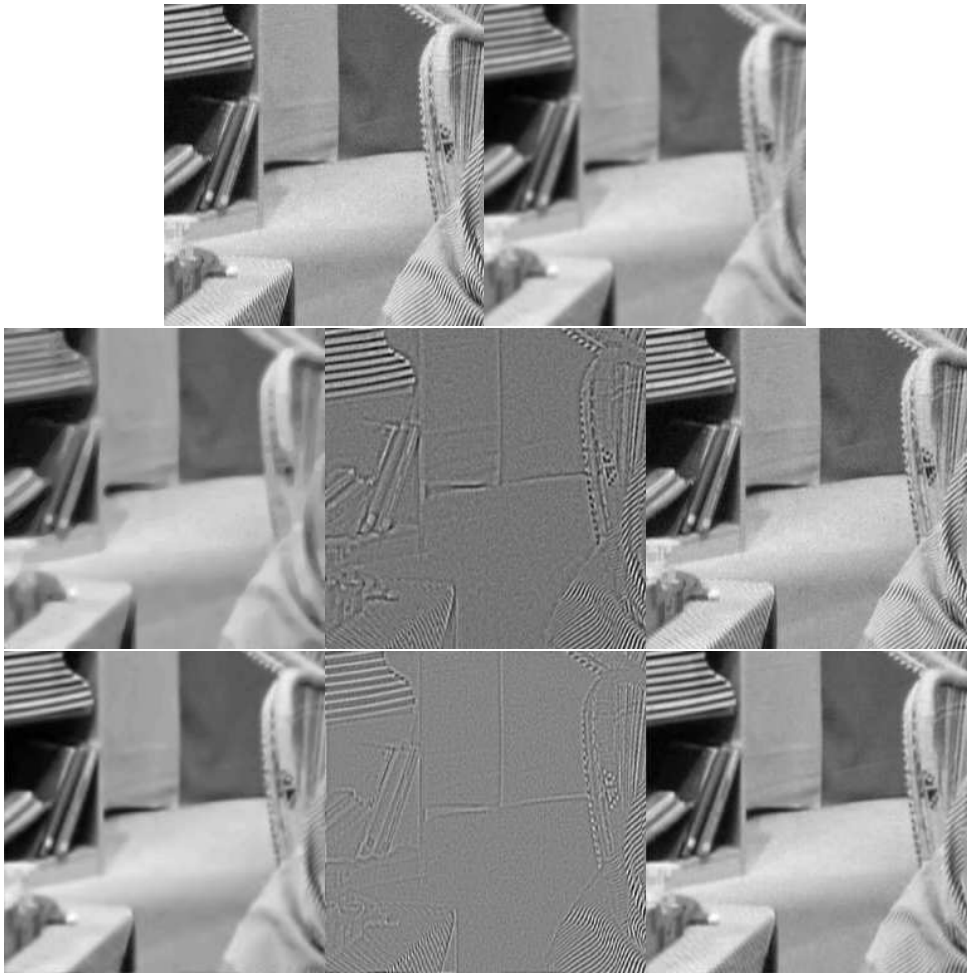

FIGURE 9. Top left: original image; top right: blurred image. Middle row (proposed BV/Sobolev model): cartoon part, texture part, recovered $u+v$ image. Bottom Row (result by Daubechies-Teschke from [12]): cartoon part, texture part, recovered $u+v$ image.

[8] G. Aubert and J. F. Aujol, *Modeling very oscillating signals. Application to image processing*, Applied Mathematics and Optimization, **51** (2005), 163–182.
[9] L. Bar, N. Kiryati and N. Sochen, *Image deblurring in the presence of impulsive noise*, International Journal of Computer Vision, **70** (2006), 279–298.
[10] L. Bar, N. Sochen and N. Kiryati, *Semi-blind image restoration via Mumford-Shah regularization*, IEEE Transactions on Image Processing, **15** (2006), 483–493.
[11] A. Chambolle and P.-L. Lions, *Image recovery via total variation minimization and related problems*, Numerische Mathematik, **76** (1997), 167–188.
[12] I. Daubechies and G. Teschke, *Variational image restoration by means of wavelets: simultaneous decomposition, deblurring, and denoising*, Applied and Computational Harmonic Analysis, **19** (2005), 1–16.
[13] I. Daubechies, G. Teschke and L. Vese, *Iteratively solving linear inverse problems under general convex constraints*, Inverse Problems and Imaging, **1** (2007), 29–46.

[14] S. Durand, F. Malgouyres and B. Rougé, *Image de-blurring, spectrum interpolation and application to satellite imaging*, ESAIM Control Optimization and Calculus of Variation, **5** (2000), 445–477.

[15] J. B. Garnett, P. W. Jones, T. M. Le and L. A. Vese, *Modeling Oscillatory Components with the Homogeneous Spaces $B\dot{M}O^{-\alpha}$ and $\dot{W}^{-\alpha,p}$*, UCLA CAM Report 07-21, 2007 (to appear in Pure and Applied Mathematics Quarterly).

[16] J. B. Garnett, T. M. Le, Y. Meyer, L. A. Vese, *Image decompositions using bounded variation and generalized homogeneous Besov spaces*, Applied and Computational Harmonic Analysis, **23** (2007), 25–56.

[17] S. Geman and D. Geman, *Stochastic relaxation, Gibbs distributions, and the Bayesian restoration of images*, IEEE Transactions on Pattern Analysis and Machine Intelligence, **6** (1984), 721–741.

[18] Y. Gousseau and J.-M. Morel, *Are natural images of bounded variation?* SIAM Journal on Mathematical Analysis, **33** (2001), 634–648.

[19] H. Fu., M. K. Ng, M. Nikolova and J. Barlow, *Efficient minimization methods of mixed $\ell 2$-$\ell 1$ and $\ell 1$-$\ell 1$ norms for image restoration*, SIAM Journal on Scientific Computing, **27** (2006), 1881–1902.

[20] Y. Kim and L. A. Vese, *Functional minimization problems in image processing*, Proc. SPIE Vol. **6814**, C. A. Bouman, E. L. Miller, I. Pollak, Editors, (2008), pages 68140Q-1–68140Q-11.

[21] T. M. Le and L. A. Vese, *Image decomposition using total variation and div(BMO)*, SIAM J. on Multiscale Modeling and Simulation, **4** (2005), 390–423.

[22] S. Levine, *An adaptive variational model for image decomposition*, LNCS, **3757** (2005), 382–397.

[23] L. Lieu, *Contribution to problems in image restoration, decomposition, and segmentation by variational methods and partial differential equations*, UCLA Ph.D. Thesis, June 2006.

[24] L. Lieu and L. Vese, *Image restoration and decomposition via bounded total variation and negative Hilbert-Sobolev spaces*, Applied Mathematics & Optimization, **58** (2008), 167–193.

[25] S. Lintner and F. Malgouyres, *Solving a variational image restoration model which involves L^∞ constraints*, Inverse Problems, **20** (2004), 815–831.

[26] F. Malgouyres, *Minimizing the total variation under a general convex constraint for image restoration*, IEEE Transactions on Image Processing, **11** (2002), 1450–1456.

[27] F. Malgouyres, *A framework for image deblurring using wavelet packet bases*, Applied and Computational Harmonic Analysis, **12** (2002), 309–331.

[28] Y. Meyer, "Oscillating Patterns in Image Processing and Nonlinear Evolution Equations," University Lecture Series, vol. **22**, Amer. Math. Soc., Providence, RI, 2001.

[29] D. Mumford and B. Gidas, *Stochastic models for generic images*, Quarterly of Applied Mathematics, **59** (2001), 85–111.

[30] S. Osher, A. Solé and L. Vese, *Image decomposition and restoration using total variation minimization and the H^{-1} norm*, Multiscale Modeling and Simulation, **1** (2003), 349–370.

[31] L. I. Rudin, S. Osher and E. Fatemi, *Nonlinear total variation based noise removal algorithms*, Physica D, **60** (1992), 259–268.

[32] L. Rudin and S. Osher, *Total variation based image restoration with free local constraints*, in "Proceedings IEEE International Conference in Image Processing," **1** (1994), 31–35.

[33] J. L. Starck, M. Elad and D. L. Donoho, *Image decomposition via the combination of sparse representations and a variational approach*, IEEE Transactions On Image Processing, **14** (2005), 1570–1582.

[34] E. Tadmor, S. Nezzar and L. Vese, *A multiscale image representation using hierarchical (BV, L^2) decompositions*, Multiscale Modeling and Simulation, **2** (2004), 554–579.

[35] E. Tadmor, S. Nezzar and L. Vese, *Multiscale hierarchical decomposition of images with applications to deblurring, denoising and segmentation*, Communications in Mathematical Sciences, **6** (2008), 281–307.

[36] H. Takeda, S. Farsiu and P. Milanfar, *Deblurring using regularized locally-adaptive kernel regression*, IEEE Transactions on Image Processing, **17** (2008), 550–563.

[37] A. N. Tikhonov, *On the stability of inverse problems*, Dokl. Akad. Nauk SSSR, **39** (1943), 195–198.

[38] A. N. Tikhonov, *Solution of incorrectly formulated problems and the regularization method*, Soviet Math Dokl 4, 1035-1038 English translation of Dokl Akad Nauk SSSR, **151** (1963), 501–504.

[39] A. N. Tikhonov and V. A. Arsenin, "Solution of Ill-posed Problems," Winston & Sons, Washington, 1977.
[40] L. Vese, *A study in the BV space of a denoising-deblurring variational problem*, Applied Mathematics and Optimization, **44** (2001), 131–161.
[41] L. A. Vese and S. J. Osher, *Modeling textures with total variation minimization and oscillating patterns in image processing*, Journal of Scientific Computing, **19** (2003), 553–572.

Received September 2008; revised November 2008.

E-mail address: yuno1123@math.ucla.edu
E-mail address: lvese@math.ucla.edu